

Supporting Information

Ligand Structure, Conformational Dynamics, and Excited-State Electron Delocalization for Control of Photoinduced Electron Transfer Rates in Synthetic Donor–Bridge–Acceptor Systems

Heather A. Meylemans, Chi-Fong Lei, and Niels H. Damrauer*

Department of Chemistry and Biochemistry, University of Colorado, Boulder, Colorado 80309

Additional Figures:

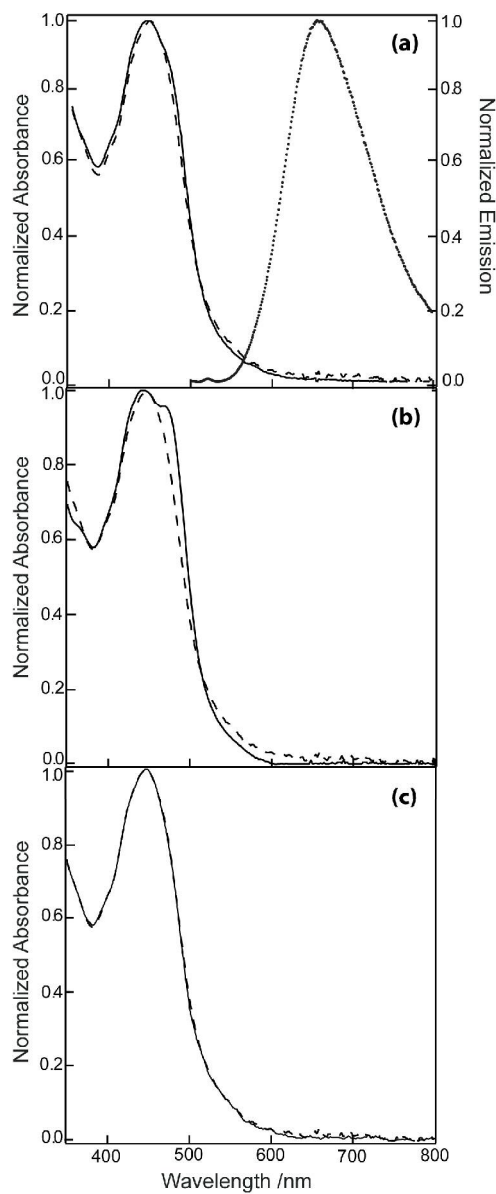


Figure S1. Normalized UV-visible absorption spectrum for **(2)** (dashed) and **(4)** (solid) in 298 K CH₃CN of various origin. **(a)** Data was collected using CH₃CN obtained from Burdick & Jackson. The emission spectrum of **(2)** collected at 298 K is also shown (dotted). **(b)** Data was collected using CH₃CN obtained from Aldrich passed through in house activated alumina stills. **(c)** Data was collected using CD₃CN obtained from Cambridge Isotope Laboratories, Inc.

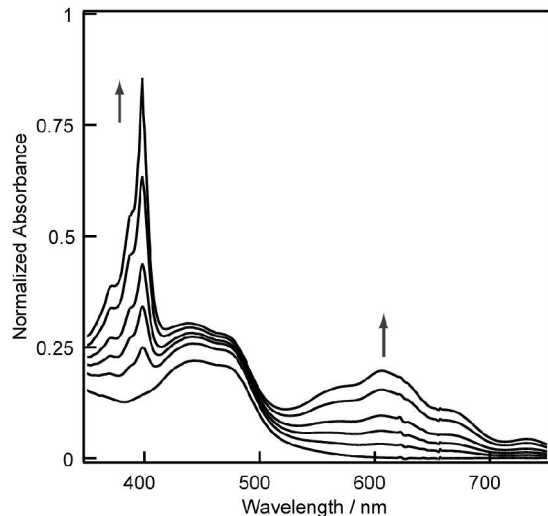


Figure S2. Spectroelectrochemical data for **(4)** recorded over a 15 min. period of bulk electrolysis with voltage held constant at -800 mV versus Ag/AgNO₃. The growth of features at 375 nm and 607 nm indicate production of reduced methyl viologen. Discontinuities at 624 nm and 657 nm are an artifact of the spectrometer and how it is blanked.

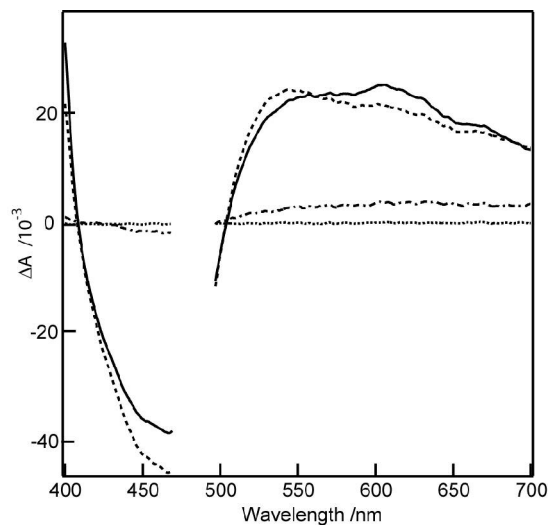
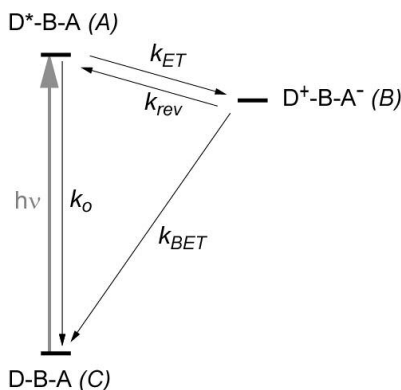


Figure S3. Transient absorption spectra for **(4)** in room temperature acetonitrile collected at -10 ps (●●), 10 ps (---), 50 ps (—), and 750 ps (◐◑) following excitation with a 480 nm, ~100 fs pump laser pulse. Data between 470 and 500 nm has been removed as it is strongly contaminated by scatter from the pump laser. These data were obtained with a ground state absorption spectrum equivalent to **Figure S1(b)**.



Scheme S1. Three-state picture used to derive the kinetics model given in Eq. 6 of the manuscript. In the model (Eq. 6), k_{rev} and k_o are ignored as they are many orders of magnitude smaller than k_{ET} or k_{BET} (see manuscript for details). The pre-exponential quantities A, B, and C are each proportional to the molar extinction coefficient of that particular species (ϵ_A , ϵ_B , or ϵ_C) with the same proportionality constant K. The proportionality constant K is a product between the initial concentration of the excited state at $t = 0$ and a factor which accounts for the effective path length in the sample which is largely dictated by the overlap between the pump and probe laser beams.

Table S1. Fitting Details for Kinetics Reported for Complexes in Room Temperature CH_3CN .

Complex (3)	607nm	594nm	440nm
y0	0.03±0.01	0.02	-0.03
A	0.621±0.007	0.625	-0.381
B	1.27±0.01	1.25	0
C	0±0	0	0.84
k1 / $10^{10} s^{-1}$	2.6±0.1	0.026	0.0263
k2 / $10^{10} s^{-1}$	0.62±0.04	0.0062	0.0062
Complex (4)	607nm	594nm	440nm
y0	0.025±0.008	0.021	-0.032
A	0.683±0.002	0.709	-0.223
B	1.49±0.02	1.47	0
C	0±0	0	0.71
k1 / $10^{10} s^{-1}$	2.8±0.02	0.028	0.028
k2 / $10^{10} s^{-1}$	1.37±0.06	0.0137	0.0137

The error bars for the parameters reported in this table represent 2σ determined from fitting three independent data sets collected for both (3) and (4) at $\lambda_{probe} = 607$ nm.

Extinction Coefficient Argument for $k_{ET} > k_{BET}$ in modeling kinetics at $\lambda_{\text{probe}} = 607$ nm.

The kinetics model we use to fit our time-resolved absorption and bleach kinetics is *Eq. 6* which is shown again below. This model is based on the three state picture shown in *Scheme S1*, where k_{rev} and k_o are negligibly small compared to k_{ET} and k_{BET} .

$$Y = Ae^{-k_{ET}t} + B \frac{k_{ET}}{k_{BET} - k_{ET}} (e^{-k_{ET}t} - e^{-k_{BET}t}) - C \left(\frac{k_{BET}}{k_{BET} - k_{ET}} e^{-k_{ET}t} - \frac{k_{ET}}{k_{BET} - k_{ET}} e^{-k_{BET}t} \right) + y_0 \quad \text{Eq. 6 from manuscript}$$

As discussed in the manuscript, this model has an inherent ambiguity. This manifests itself in the fact that the shape of the kinetics (for example a rising feature with time followed by a decay) are not sufficient information to determine whether $k_{ET} > k_{BET}$ (*case 1*) or whether $k_{BET} > k_{ET}$ (*case 2*). In essence, absent a priori knowledge of individual rate constants or pre-exponential quantities, the data can be modeled in two different ways ($k_{ET} > k_{BET}$ (*case 1*) or $k_{BET} > k_{ET}$ (*case 2*)) with equal quality in the least squares fitting. Additional information/analysis is needed to distinguish between the two cases.

We have analyzed our fit coefficients for **(3)** and **(4)** with the gross assumptions that the extinction coefficient for $D^+ - B - A^-$ at $\lambda_{\text{probe}} = 607$ nm is due only to the reduced methyl viologen and that the bleach feature at early times are pure (i.e., due only to loss of the ground state absorbance). Under these circumstances we obtain good agreement for *case 1* (where $k_{ET} > k_{BET}$) for **(4)**. For **(3)** the same analysis is inconclusive but at the same time does not favor *case 2* (where $k_{BET} > k_{ET}$). As discussed in the manuscript, the strongest arguments for $k_{ET} > k_{BET}$ come from our analysis/interpretation of the electron transfer phenomena themselves.

The general kinetics model given in *Eq. 6* contains pre-exponential quantities A , B , and C which relate to each of the possible species in kinetic evolution of these photoexcited $D - B - A$ systems (see *Scheme S1*): $D - B - A$ (C), $D^* - B - A$ (A), and $D^+ - B - A^-$ (B). The quantities A , B , and C are each proportional to the molar extinction coefficient of that particular species (ϵ_A , ϵ_B , or ϵ_C) with the same proportionality constant K . For example, $A = K \times \epsilon_A$, $B = K \times \epsilon_B$, and $C = K \times \epsilon_C$. The proportionality constant K is a product between the initial concentration of the excited state at $t = 0$ and a factor which accounts for the effective path length in the sample which is largely dictated by the overlap between the pump and probe laser beams. The quantity K is difficult to know exactly but as described below, it is not important for our purposes.

For data collected at $\lambda_{\text{probe}} = 607$ nm, $C = 0$ because the ground state does not absorb at this wavelength. In estimating the extinction coefficient associated with B ($D^+ - B - A^-$), we need information about the reduced methyl viologen acceptor. The extinction coefficient for reduced methyl viologen at 607nm was previously reported as $13,900 \text{ cm}^{-1}\text{M}^{-1}$ (see ref 112 of the manuscript). Therefore in the analysis below $\epsilon_B = 13,900 \text{ cm}^{-1}\text{M}^{-1}$.

The value of ϵ_A (at $\lambda_{\text{probe}} = 607$ nm) in **(3)** and **(4)** can be estimated using separate data, namely, transient absorption spectra collected at early times before electron transfer has taken place (e.g., $t = 1$ ps following photoexcitation (data not shown)). If we assume the bleach is relatively pure (i.e., just loss of ground state absorbance) we can ratio the magnitude of the transient absorption at $\lambda_{\text{probe}} = 607$ nm to the magnitude of the bleach at $\lambda = 455$ nm for **(3)** and $\lambda = 444$ nm for **(4)**. These bleach wavelengths are chosen because we know the molar extinction coefficient for **(3)** and **(4)** at that respective wavelength (see *Table 1*). For **(3)** at $\Delta t = 1$ ps the magnitude of the absorbance at $\lambda_{\text{probe}} = 607$ nm is 30% of the magnitude of the bleach at $\lambda_{\text{probe}} = 455$ nm providing an estimate of $\epsilon_A = 4600 \text{ cm}^{-1}\text{M}^{-1}$. From this we compute a ratio $\epsilon_A/\epsilon_B = A/B =$

4600 cm⁻¹ M⁻¹/ 13900 cm⁻¹ M⁻¹ = 0.33. For **(4)** at $\Delta t = 1$ ps we observe the magnitude of the absorbance at $\lambda_{\text{probe}} = 607$ nm is 40% of the magnitude of the bleach at $\lambda_{\text{probe}} = 444$ nm providing an estimate of $\epsilon_A = 6000$ cm⁻¹ M⁻¹. For this species we compute the ratio $\epsilon_A/\epsilon_B = A/B = 6000$ cm⁻¹ M⁻¹/ 13900 cm⁻¹ M⁻¹ = 0.43. These estimated values for A/B are listed below in **Table S2** as ‘Expected A/B’.

We can now fit the $\lambda_{\text{probe}} = 607$ nm data for **(3)** and **(4)** under the two circumstances: *case 1* where $k_{ET} > k_{BET}$ and *case 2* where $k_{BET} > k_{ET}$. Values for the coefficients A and B that are obtained (the average of three independent measurements; see **Table S1**) are listed in **Table S2**.

Table S2. Fit comparison for two kinetics model cases.

Complex	B	A	A/B	Expected A/B
(3) <i>case 1</i> : $k_{ET} > k_{BET}$	1.27	0.621	0.49	0.33
(3) <i>case 2</i> : $k_{BET} > k_{ET}$	3.29	0.630	0.19	
(4) <i>case 1</i> : $k_{ET} > k_{BET}$	1.49	0.683	0.46	0.43
(4) <i>case 2</i> : $k_{BET} > k_{ET}$	2.38	0.677	0.28	

As seen in the comparison of A/B from the fits to the ‘Expected A/B’, there is very good agreement for **(4)** under the circumstances of *case 1* where $k_{ET} > k_{BET}$ (0.46 from the fit versus the expected 0.43). For **(3)** the analysis does not favor either case and therefore cannot be used to rule out *case 2*. At this point we do not have a good explanation why the gross model is sufficient for **(4)** but not **(3)**. As argued below, ϵ_A and ϵ_B are not well known at this time for either species.

We do not think it is reasonable to invoke the possibility that one of the molecules behaves according to *case 1* while the other behaves according to *case 2*. Under these circumstances it would be very difficult to invoke a self-consistent mechanistic picture that explains the driving-force dependence of for k_{ET} and k_{BET} for **(3)** versus **(4)**. It would lead to a situation where Marcus theory predictions of driving force dependence in either the normal or inverted region are called into question.

We stress here that a careful analysis of fit coefficients requires quantities whose value is unknown at this time and difficult to obtain with sufficient certainty to make arguments for *case 1* or *case 2* bulletproof. As discussed above, the first quantity needed is the extinction coefficient due to D^+-B-A^- at $\lambda_{\text{probe}} = 607$ nm for both **(3)** and **(4)**. While the extinction coefficient for reduced methyl viologen has been reported (see ref 112 of the manuscript) we do not know the contribution to absorbance due to the oxidized metal center. The oxidized donor species would be absorptive at 607 nm based on spectroelectrochemical data previously reported for similar compounds (see ref 56 of the manuscript). Second, we need to know the relative absorbance at $\lambda_{\text{probe}} = 607$ nm due to D^*-B-A prior to electron transfer. If bleach features seen in transient difference spectra at early times for **(3)** and **(4)** are pure, i.e., are due only to loss of ground state absorbance, this information would be available. However, Creutz et al. (*JACS* **1980**, 102, 1309) have shown that in the ³MLCT excited state of the parent complex $[\text{Ru}(\text{bpy})_3]^{2+}$, the bleach wavelengths of typical excited-state difference spectra are convoluted with excited-state absorbances presumably due to the formally reduced ligand species. Undoubtedly this would also be true for **(3)** and **(4)**. Until the extinction coefficient for these excited state species in **(3)** and **(4)** are known, we cannot accurately know an extinction coefficient for D^*-B-A at $\lambda_{\text{probe}} = 607$ nm for these two molecules. Of course the same measurements needed to determine

extinction coefficients for the $^3\text{MLCT}$ excited state at bleach wavelengths could be used to directly measure extinction coefficients at $\lambda_{\text{probe}} = 607$ nm.

Again we stress that the strongest evidence for *case 1* where $k_{ET} > k_{BET}$ for **(3)** and **(4)** lies in our analysis/interpretation of the electron transfer rate constants as described in the manuscript.